International Journal of Computer Applications in Engineering Sciences
[VOL I, ISSUE II, JUNE 2011] [ISSN: 2231-4946]

Efficient Feature Analysis of Radiographs in Bone Age Assessment

P.Thangam[#], K.Thanushkodi[*], T.V.Mahendiran[$]

[#]*Department of CSE(PG), Sri Ramakrishna Engineering College, Coimbatore, Tamilnadu, India*
[*]*Akshaya College of Engineering and Technology, Coimbatore, Tamilnadu, India*
[$]*Department of EEE, Coimbatore Institute of Engineering and Technology, Coimbatore, India.*

[#]saithangam@gmail.com, [*]thanush12@gmail.com, [$]saimahegobi@gmail.com

***Abstract*— This paper presents the development procedure of feature extraction and analysis of the features extracted from left hand wrist radiographs, which could be further used in estimating the skeletal maturity or bone age. Bone Age Assessment (BAA) is a procedure used in the management and diagnosis of endocrine disorders. It also serves as an indication of the therapeutic effect of treatment. It is of much significance in pediatric medicine in the detection of hormonal growth or even genetic disorders. In the proposed work, the input radiographs are first preprocessed and segmented using a Particle Swarm Optimization (PSO) based segmentation algorithm using Tetrolets, to identify the wrist bones which form the Regions of Interest (ROIs). The identified ROIs are broadly categorized into Carpal bones and Phalangeal bones. From the ROIs, 47 features that describe the morphology of the bones are extracted. Since it will be infeasible for a classifier to handle such a huge number of features, PCA is employed as a tool for feature analysis and thereafter for feature selection. PCA reduces the dimensionality of the features to produce a powerful yet concise feature vector. The results on both the carpal and the phalangeal bones are discussed and the features surpassing the analysis strategy are highlighted.**

***Keywords* — Bone age assessment (BAA), Particle Swarm Optimization (PSO), Tetrolets, Principal Component Analysis (PCA), Region of Interest (ROI).**

I. INTRODUCTION

The chronological situations of humans are described by certain indices such as height, dental age, and bone maturity. Of these, bone age measurement plays a significant role because of its reliability and practicability in diagnosing hereditary diseases and growth disorders. Bone age assessment using a hand radiograph is an important clinical tool in the area of pediatrics, especially in relation to endocrinological problems and growth disorders. A single reading of skeletal age informs the clinician about the relative maturity of a patient at a particular time in his or her life and integrated with other clinical finding, separates the normal from the relatively advanced or retarded [1]. The bone age of children is apparently influenced by gender, race, nutrition status, living environments and social resources, etc. Based on a radiological examination of skeletal development of the left-hand wrist, bone age is assessed and compared with the chronological age. A discrepancy between these two values indicates abnormalities in skeletal development. The procedure is often used in the management and diagnosis of endocrine disorders and also serves as an indication of the therapeutic effect of treatment. It indicates whether the growth of a patient is accelerating or decreasing, based on which the patient can be treated with growth hormones. BAA is universally used due to its simplicity, minimal radiation exposure, and the availability of multiple ossification centers for evaluation of maturity.

II. BACKGROUND OF BAA

The main clinical methods for skeletal bone age estimation are the Greulich & Pyle (GP) method and the Tanner & Whitehouse (TW) method. GP is an atlas matching method while TW is a score assigning method [2]. GP method is faster and easier to use than the TW method. Bull et. al. performed a large scale comparison of the GP and TW method and concluded that TW method is the more reproducible of the two and potentially more accurate [3].

In GP method, a left-hand wrist radiograph is compared with a series of radiographs grouped in the atlas according to age and sex. TW method uses a detailed analysis of each individual bone, assigning it to one of eight classes reflecting its developmental stage. This leads to the description of each bone in terms of scores. The sum of all scores assesses the bone age. Fig. 1 shows the development of the radius bone into stages (A,B,C,D,…I) as:

- Stage A – absent
- Stage B – single deposit of calcium
- Stage C – center is distinct in appearance
- Stage D – maximum diameter is half or more the width of metaphysis
- Stage E – border of the epiphysis is concave

- Stage F – epiphysis is as wide as metaphysis
- Stage G – epiphysis caps the metaphysis
- Stage H – fusion of epiphysis and metaphysis has begun
- Stage I – epiphyseal fusion completed.

By adding the scores of all ROIs, an overall maturity score is obtained. This score is correlated with the bone age differently for males and females [4].

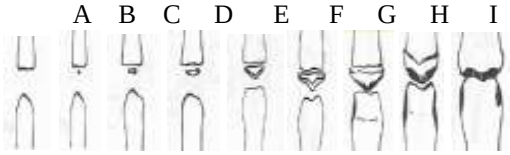

Fig. 1. TW stages of phalanx bone

III. System Design

The system consists of four modules, namely:

1. Image Pre-processing
2. Edge Detection and Segmentation
3. Feature Extraction
4. Feature Analysis and Selection

A. Image Preprocessing:

Image preprocessing is performed in two steps: Image smoothing, and Grayscale conversion. Image smoothing is done to reduce the noise within the image or to produce a less pixilated image. Most smoothing methods are based on low pass filters. In our system, we have done smoothing to reduce noise by using a Gaussian filter. Gaussian filter reduces the magnitude of higher frequencies proportional to the lower frequencies, but at the cost of more computation time. But the speeding up of smoothing is achieved by splitting *2D* Gaussian *G(x,y)* into two *1D* Gaussians *G(x)G(y)* and carrying out filtering in *1D*, first row by row and then column by column. Grayscale conversion is done as follows. Colors in an image are converted to a shade of gray by calculating the effective brightness or luminance of the color and using this to create a shade of gray that matches the desired brightness.

B. Edge Detection and Segmentation:

We have made use of Sobel edge detector to detect the edges. The Sobel operator performs a *2D* spatial gradient measurement on an image. Typically it is used to find the approximate absolute gradient magnitude at each point in an input grayscale image. The Sobel edge detector uses a pair of 3 x 3 convolution masks, one estimating the gradient in the *x*-direction (columns) and the other estimating the gradient in the *y*-direction (rows). A convolution mask is usually much smaller than the actual image. As a result, the mask is slid over the image, manipulating a square of pixels at a time. The actual Sobel masks [5] are given below:

-1	0	+1
-2	0	+2
-1	0	+1

Gx

+1	+2	+1
0	0	0
-1	-2	-1

Gy

The magnitude of the gradient is then calculated using the formula:

$$|G| = \sqrt{G_x^2 + G_y^2} \quad (1)$$

An approximate magnitude can be calculated using:

$$|G| = |Gx| + |Gy| \quad (2)$$

Tetrolet-based segmentation method proposed in this paper, makes use of tetrolets for decomposing the input image into sparse representation. The decomposed tetrolet co-efficients [6] are fed as particle solutions to the PSO segmentation algorithm. The algorithm segments the input left hand wrist radiograph and identifies the ROIs for further computations.

3.2.1 Decomposition into Tetrolets:

1. The image a^{r-1} is divided into blocks $Q_{i,j}$ of size 4 x 4, $i, j = 0, \ldots N/4^r - 1$.
2. In each block Qi,j, the 117 admissible tetromino coverings $c = 1, \ldots, 117$ are considered.

For each tiling c, a Haar wavelet transform is applied to the four tetromino subsets $I^{(c)}_s$, $s = 0, 1, 2, 3$. In this way, for each tiling c, four low-pass coefficients and 12 tetrolet coefficients are obtained. In Qi,j, the pixel averages for every admissible tetromino configuration $c = 1, \ldots, 117$ by equation (3) and the three high-pass parts for $l = 1,2,3$ given by equation (4) respectively:

$$a^{r,(c)} = \left(a^{r,(c)}[s]\right)_{s=0}^{3} \text{ with } a^{r,(c)}[s] = \sum_{(m,n)\in I_s^{(c)}} \varepsilon[0, L(m,n)]\, a^{r-1}[m,n] \quad (3)$$

$$w_l^{r,(c)} = \left(w_l^{r,(c)}[s]\right)_{s=0}^{3} \text{ with } w_l^{r,(c)}[s] = \sum_{(m,n)\in I_s^{(c)}} \varepsilon[l, L(m,n)]\, a^{r-1}[m,n] \quad (4)$$

where the coefficients ε[l,m], l,m = 0, . . . , 3, are entries from the Haar wavelet transform matrix:

$$W := \left(\varepsilon[l,m]\right)_{l,m=0}^{3} = \frac{1}{2}\begin{pmatrix} 1 & 1 & 1 & 1 \\ 1 & 1 & -1 & -1 \\ 1 & -1 & 1 & -1 \\ 1 & -1 & -1 & 1 \end{pmatrix} \quad (5)$$

3. The low- and high-pass coefficients of each block are re-arranged into a 2 x 2 block.
4. The tetrolet coefficients (high-pass part) are stored.

5. Step 1 to 4 is applied to the low-pass image.
6. The tetrolet coefficients are fed as input to the PSO algorithm.
7. The segmented bones are output.

3.2.2 Overview of PSO:

Particle Swarm Optimization (PSO) is an algorithm for finding optimal regions of complex search space through interaction of individuals in a population of particles. PSO algorithm, originally introduced in terms of social and cognitive behavior by Eberhart and Kennedy [7] has been proven to be a powerful competitor to other evolutionary algorithms such as genetic algorithms. PSO is a population based stochastic optimization technique and well adapted to the optimization of nonlinear functions in multidimensional space [8]. PSO algorithm simulates social behavior among individuals (particles) flying through multidimensional search space, each particle representing a single intersection of all search dimensions [9]. The particles evaluate their positions relative to a global fitness at every iteration, and companion particles share memories of their best positions, and then use those memories to adjust their own velocities and positions. At each generation, the velocity of each particle is updated, being pulled in the direction of its own previous best solution (local) and the best of all positions (global) [10,11]. Computation of optimal threshold is handled here with Particle Swarm Optimization (PSO). There are six important control parameters in PSO algorithm. They are: Population Size, Cognitive Learning Rate, Social Learning Rate, Maximum of Particle Flying Speed, Inertia Weight factor, and Constriction factor. The population size of particles refers the number of particles in iterative process, thus denoting components in the image here. A population of particles is initialized with random positions and velocities in d-dimensional space. A fitness function, f is evaluated, using the particle's positional coordinates as input values. Positions and velocities are adjusted, and the function is evaluated with the new coordinates at each time-step.

Algorithm

Step 1: In every iteration, each particle is updated by following two "best" values, Personal best and Global best.

Step 2: After finding the two best values, the particle updates its velocity and positions with following equation (6) and (7)

$$v[i]=v[i]+c1*rand(i)*(pbest[i] - present[i]) + c2*rand(i)*(gbest[i]–present[i]) \quad (6)$$

$$present[i]=present[i]+v[i] \quad (7)$$

v[i] is the particle velocity, *present[i]* is the current particle (solution), *pbest[i]* and *gbest[i]* are defined as stated before, *rand(i)* is a random number between *(0,1)* and *c1, c2* are learning factors. Usually *c1=c2=2*.

3.2.3. Implementation of PSO for tetrolet-based segmentation:

The implementation of the segmentation algorithm consists of the following steps.

Step 1: *Swarm Formation:* For a population size *p*, the particles are randomly generated between the minimum and the maximum limits of the threshold values.

Step 2: *Objective Function evaluation:* The objective function values of the particles are evaluated.

Step 3: *' pbest' and 'gbest' initialization:* The objective values obtained above for the initial particles of the swarm are set as the initial *pbest* values of the particles. The best value among all the *pbest* values is identified as *gbest*.

Step 4: *Velocity computation:* The new *velocity* for each particle is computed using equation (6).

Step 5: *Position computation:* The new *position* for each particle is computed using equation (7).

Step 6: *Swarm Updation:* The values of the objective function are calculated for the updated positions of the particles. If the new value is better than the previous *pbest*, the new value is set to *pbest*. Similarly, *gbest* value is also updated as the best pbest.

Step 7: *Termination:* If the stopping criteria are met, the positions of particles represented by *gbest* are the optimal threshold values. Otherwise, the procedure is repeated from step 4.

C. Feature Extraction:

Feature extraction is performed as a way to reduce the dimensionality of the data. A long list of candidate features was calculated in order to form a powerful input vector. The features attempted to describe the morphology of the outline shape of the bones (ROIs). Once extracted and optimized, the vector would be used to train and validate the classifier. The list of candidate features are categorized into two groups, based on the ROIs they are extracted from, as:

groups, based on the ROIs they are extracted from, as:

1. Carpal features: (8 features)
   - *BRlength*
   - *BRwidth*
   - *BRdiagonal*
   - *BRarea*
   - *BRperimeter*
   - *INarea*
   - *INperimeter*
   - *BR_INratio*
2. Phalangeal features: (3 + 12 x 3 = 39)
   - *MedianLength* (3 fingers)

DistalValues (3 fingers)
- *DistalLength*
- *DistalWidth*
- *DistalArea*
- *DistalPerimeter*

MiddleValues (3 fingers)
- *MiddleLength*
- *MiddleWidth*
- *MiddleArea*
- *MiddlePerimeter*

ProximalValues (3 fingers)
- *ProximalLength*
- *ProximalWidth*
- *ProximalArea*
- *ProximalPerimeter*

3.3.1. Carpal Features:

For the carpal bones, all the carpal bones are together identified as an inner region and are enclosed inside a bounding rectangle. Five features, namely the length, width, area, perimeter and the diagonal length of the bounding rectangle are calculated. The length and width are calculated as the sum of pixels along the boundary. The area, perimeter and diagonal are given by,

$$Area = Length \times Width \tag{8}$$

$$Perimeter = 2 \times Length + 2 \times Width \tag{9}$$

$$Diagonal = \sqrt{Length^2 + Width^2} \tag{10}$$

For the inner region of carpals, two features namely the inner area and perimeter are calculated as the number of pixels enclosed within the boundaries, and along the boundaries of the sample region respectively. The last carpal feature is the ratio between the outer and inner areas given by,

$$BR\_INratio = \frac{BRarea}{INarea} \tag{11}$$

Thus, a total of 8 carpal features are extracted. Fig. 2 provides a snapshot of the input, edge detected and the segmented images. Fig. 3 provides the snapshot of extracting the carpal ROI features.

(a) (b) (c)

Fig. 2. (a) Pre-processed image (b) Edge detected image (c) Segmented image

(a) (b) (c)

Fig. 3. (a) Carpal ROI (b) Region Fill (c) Inner region

3.3.2. Phalangeal Features:

Phalangeal features are extracted from three fingers, namely the index, middle and third finger. For each finger, the three phalangeal bones: distal, middle and proximal are considered and from each of them four features are extracted (length, width, area, perimeter). Also the length of the median for the finger phalanges is calculated for each finger. Thus, 13 features are extracted from each finger and hence the total number of phalangeal features is 39. Fig. 4 provides the snapshot of extracting and cropping the phalangeal ROI. Fig. 5 shows the extraction of features from the distal, middle and proximal phalanges individually and Fig. 6 shows the extraction of *MedianLength* feature.

D. Feature Analysis and Selection:

Totally 47 features are extracted from the segmented bones of the left hand wrist radiograph, producing a multi-dimensional set of data. It is impractical to feed data of such high dimensionality into a classifier. The exploration of the data set can give a valuable insight of the expected behavior of the end system and therefore assist further improvement of its performance[12].

3.4.1 PCA:

The extracted features are analyzed using Principal Component Analysis (PCA), thus reducing the feature vector into 11 important features. PCA [13-15] is a vector space transformation often used to reduce multidimensional datasets to lower dimensions for analysis. Given data X consisting of N samples, PCA first performs data normalization by subtracting the mean vector m from the data. Then the covariance matrix Σ of the normalized data $(X - m)$ is computed.

$$m = \frac{1}{N} \sum_{i=1}^{N} X_i \tag{12}$$

$$\sum = (X - m)(X - m)^T \tag{13}$$

Afterwards, the basis functions are obtained by solving the algebraic eigen value problem

$$\Lambda = \Phi^T \sum \Phi \qquad (14)$$

where Φ is the eigen vector matrix of Σ, and Λ is the corresponding diagonal matrix of eigen values. Feature selection is then performed by keeping q ($q < N$) orthonormal eigen vectors corresponding to the first q largest eigen values of the covariance matrix.

(a) (b)

Fig. 4. (a) Phalangeal ROI (b) Cropped region

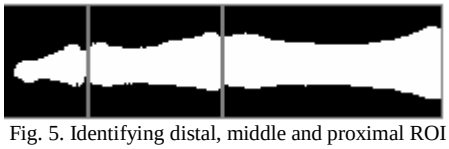

Fig. 5. Identifying distal, middle and proximal ROI

Fig. 6. Extracting Length of median

3.4.2 Feature Selection:

The features that surpass the others in feature analysis are found to be the principal components. Those features are selected for further processing, discarding the lagging ones. The features selected in our system are:

1. *BRperimeter*
2. *BRarea*
3. *INarea*
4. *BR_INratio*
5. *MedianLength*
6. *DistalArea*
7. *DistalPerimeter*
8. *MiddleArea*
9. *MiddlePerimeter*
10. *ProximalArea* and
11. *ProximalPerimeter*.

Thus the feature vector is reduced from 47 features to 11 features that contribute better in the bone age estimation process.

IV. Results And Discussion

The system was tested with 100 left hand wrist images (50 males and 50 females). The quality of the segmentation was influenced by the image quality. For radiographs over exposed to radiation, further preprocessing was required, to achieve good results. The use of image pre-processing techniques such as image smoothing and gray scale conversion improved the quality of the digitized radiograph. The noise caused due to radiation and other external factors were eliminated. Sobel edge detector identified the boundary of the bones or ROIs. Then, PSO algorithm for tetrolet-based image segmentation was applied to segment the bones from the radiograph. The segmentation was regarded as accurate if the sum of over selected and under selected pixels were less than 25. The segmentation process was accurate by 0.94 for males and 0.96 for females, as tabulated in Table I. From the segmented bones, the Carpal and Phalangeal ROI were identified and used for feature extraction. A list of 47 features was extracted from these ROIs. The extracted features were subjected to PCA thus reducing the feature vector size into 11 important contributing features. Table II represents the accuracy of feature extraction for the discriminating features. From the analysis, the following are inferred:

- The carpal features contribute more during the earlier classes of the age group 1-10, while phalangeal features contribute much during the latter classes.
- Hence, carpal and phalangeal bones are more important to be considered for BAA process.
- The growth of carpal bones seems to be more rapid in girls, while it is gradual and slow in boys.
- The growth of the phalangeal bones is gradual both in boys and girls, at the same time their growth seem to be dominant in boys rather than in girls.
- When considering similarity, the *MedianLength* feature from the phalanges showed similar values for boys and girls.
- Much difference is encountered between boys and girls in the ossification of the phalanges, thus showing significant disparity in the features *ProximalArea and ProximalPerimeter*.

TABLE I: ACCURACY OF SEGMENTATION

Sex	No. of Images	Accurate	Inaccurate	Accuracy
Male	50	47	3	94%
Female	50	48	2	96%

TABLE II: ACCURACY OF FEATURE EXTRACTION

	BR	Distal	Middle	Proximal	Carpal (Inner)
Area	100%	98%	96%	90%	86%
Perimeter	100%	96%	95%	88%	82%

V. CONCLUSION

The work presents an efficient method for segmenting wrist bones from left hand wrist radiographs and feature extraction, which can be further used for skeletal bone age assessment. The input image was first pre-processed to remove noise and was grayscale converted to improve image quality. Sobel edge detector was used for edge detection and then PSO combined tetrolet-based segmentation was performed. From the segmented bones, the carpal and phalangeal ROIs were identified and 47 features were extracted from the ROI. The extracted features were analyzed and subjected to PCA and were reduced in dimensionality into a feature space of 11 features. The system was evaluated with 100 left hand wrist images (50 males and 50 females) and the results were discussed. Future work would regard utilizing the extracted features for further computations in assessing the bone age, which is the second phase of the research project.

REFERENCES

[1] Vicente Gilsanz, and Osman Ratib, Hand Bone Age – A Digital Atlas of Skeletal Maturity, (Springer-Verlag, 2005).

[2] Concetto Spampinato, Skeletal Bone Age Assessment, University of Catania, Viale Andrea Doria, 6 95125, 1995.

[3] R.K.Bull, P.D.Edwards, P.M.Kemp, S.Fry, I.A.Hughes, Bone Age Assessment: a large scale comparison of the Greulich and Pyle, and Tanner and Whitehouse (TW2) methods, Arch. Dis. Child, vol.81, pp. 172-173, 1999.

[4] J.M.Tanner, R.H.Whitehouse, Assessment of Skeletal Maturity and Prediction of Adult Height (TW2 method), (Academic Press, 1975).

[5] Rafael C.Gonzalez, Richard E. Woods, Digital Image Processing, Third Edition, (Pearson, 2009).

[6] Jens Krommweh, Tetrolet Transform: A New Adaptive Haar Wavelet Algorithm for Sparse Image Representation", J.Vis. Commun. (2010), doi:10.1016/j.jvcir.2010.02.011.

[7] J. Kennedy, and R.C. Eberhart, "Particle Swarm Optimization," Proc of the IEEE International Conference on Neural Networks, Australia, pp. 1942–1948. 1995.

[8] J.Kennedy, R.C.Eberhart, Y.Shi, Swarm Intelligence, Morgan Kaufmann Publishers, 2001.

[9] Nadia Nedjah, Luiza de Macedo Mourelle, Swarm Intelligent Systems, Springer, 2006.

[10] http://www.swarmintelligence.org/

[11] http://www.particleswarm.info/

[12] Lefkaditis, D., Awcock, G. J. & Howlett, R. J., Intelligent Optical Otolith Classification for Species Recognition of Bony Fish, in International Conference on Knowledge-Based & Intelligent Information & Engineering Systems, Bournemouth, UK: Springer-Verlag, pp. 1226-1233, 2006.

[13] Lindsay I Smith, A Tutorial on Principal Component Analysis, Feb 2002.

[14] Christopher J.C. Burges, Geometric Methods for Feature Extraction and Dimensional Reduction, (Microsoft Research).

[15] Mark S. Nixon and Alberto S. Aguado, Feature Extraction and Image Processing, (Newnes, 2002).